

# An efficient hardware-aware matrix-free implementation for finite-element discretized matrix-multivector products

Gourab Panigrahi\*, Nikhil Kodali\*, Debashis Panda, Phani Motamarri†  
Department of Computational and Data Sciences  
Indian Institute of Science, Bangalore, India

**Abstract**—Recent hardware-aware algorithms for finite-element (FE) discretized matrix-vector multiplications suggest that on-the-fly matrix-vector products reduce arithmetic complexity and data access costs. These matrix-free approaches rely on the tensor-structured nature of the FE polynomial basis for evaluating the underlying integrals without explicitly building the global sparse matrix. The current state-of-the-art implementations of such matrix-free algorithms deal with the action of FE discretized matrix on a single vector and are not readily applicable for matrix multivector products involving large number of vectors. We propose a computationally efficient and scalable matrix-free implementation procedure to compute FE discretized matrix-multivector products on both multi-node CPU and GPU architectures.

## I. INTRODUCTION

Finite-element (FE) based numerical approaches are routinely employed to solve partial differential equations arising in various areas of science and engineering. The finite-element (FE) discretization of a partial differential equation usually involves the construction of a FE discretized operator and often requires computing its action on trial FE discretized fields for the solution of a linear system of equations or eigenvalue problems (usually utilizing iterative solvers). The evaluation of this product of the sparse matrix (FE discretized operator) and the vector (FE discretized field) is usually the computationally demanding step and is traditionally computed by using sparse-matrix vector multiplication modules. Previously, it has been noted that the evaluation of such sparse matrix-vector products can be done more efficiently on multithreaded architectures using cell-level dense matrix-vector multiplications followed by the assembly of cell-level product vectors [1]. This strategy has been recently employed on multi-node CPUs and GPUs, where evaluating the cell-level dense matrix-multivector products involving large number of vectors ( $>300$ ), demonstrated good throughput performance [2] [3] for the solution of FE discretized large-scale nonlinear eigenvalue problems arising in the quantum modelling of materials using density functional theory. However, recent hardware-aware algorithms for evaluating such matrix-vector multiplications suggest that on-the-fly matrix-vector products without storing the cell-level dense matrices reduce both arithmetic complexity and memory footprint [4] [5] [6]. These are referred to as matrix-free approaches which

exploit the tensor-structured nature of the finite-element basis functions and recast the 3D integrals involved in the matrix-vector products as a sequence of tensor contractions.

Currently available open-source implementations of the above matrix-free methods [7] [8] [9] are neither optimal nor directly applicable for the action of a FE discretized operator on large number of multiple FE discretized fields. Such situations are often encountered in solving FE discretized eigenvalue problems [10] using iterative orthogonal projection approaches or solving linear system of equations arising from FE discretizations with multiple RHS vectors. These kinds of problems arise in real-space quantum modeling of materials [11] [3] [12] or in scientific machine learning to train ML models with the solutions of FE discretized partial differential equations with multiple forcing vectors [13]. Although some preliminary work [14] [15] exists in this regard, no widely available implementation procedures exist for performing generic FE discretized matrix-multivector efficiently under the matrix-free paradigm.

This work proposes an efficient hardware-aware implementation procedure for the matrix-free algorithm to compute such FE discretized matrix-multivector products on both CPU only and GPU architectures. We first present a data layout for storing the FE discretized global multivector to minimize the non-contiguous data accesses during the extraction of the cell-level vector from the global vector resulting in efficient parallelization. Furthermore, we employ optimized small matrix multiplication routines using Just-In-Time (JIT) code generation [16] [17] on CPU only architectures to perform the underlying tensor contractions. On GPU based architectures, the proposed matrix-free implementation utilizes the concept of kernel fusion to minimize data access and efficiently utilizes the GPU shared memory and registers to pipeline data access and computation.

We assess the performance of our implementation on a representative FE discretized matrix. To this end, we choose FE basis overlap (mass) matrix times multivector multiplications as our model problem. Our investigations reveal superior performance of the proposed implementation. For instance, computational gains of up to 2.9x on GPUs and 6.12x on CPUs for matrix-multivector products using the proposed implementation when compared to the FE cell-level matrix-multiplication approach for 100 vectors. We further benchmark our performance against the deal.II [7] library and observe

Gourab Panigrahi and Nikhil Kodali contributed equally to the work.

† Corresponding author: phanim@iisc.ac.in

speedups up to 2x for multivectors on CPU only architectures and 1.4x on GPUs for 100 vectors. We also present a strong scaling study of our proposed implementation both multinode CPU and GPU architectures. The proposed implementation can be straightforwardly extended to FE discretized Laplacian and Helmholtz operators.

## II. BACKGROUND

For a generic finite-element (FE) discretized operator  $\mathbf{A}$  in 3D, the matrix-free method for computing the matrix-vector product  $\mathbf{A}\mathbf{u}$  relies on the computation of the cell level product  $(\mathbf{A}\mathbf{u})^{(e)}$  usually employing the Gauss-Legendre quadrature rule for evaluating the underlying integrals corresponding to a given FE cell  $(e)$  as shown below:

$$\begin{aligned} (\mathbf{A}\mathbf{u})_i^{(e)} &= \sum_{j=1}^{D_e} A_{ij}^{(e)} u_j^{(e)} \\ &= \sum_{j,q} \left[ F \left( \phi_i(\boldsymbol{\xi}_q), \mathbf{J}^{(e)-1} \nabla \phi_i(\boldsymbol{\xi}_q), \phi_j(\boldsymbol{\xi}_q) \mathbf{J}^{(e)-1} \nabla \phi_j(\boldsymbol{\xi}_q) \right) \right. \\ &\quad \left. w_q \det(\mathbf{J}^{(e)}) u_j^e \right], \quad \text{with } i = 1, \dots, D_e \end{aligned} \quad (1)$$

where  $D_e$  denotes the number of degrees of freedom for the given FE cell  $(e)$  and  $\phi_i(\boldsymbol{\xi})$  denotes the  $i^{\text{th}}$  cell-level FE polynomial basis function in the natural coordinate system  $\boldsymbol{\xi} = (\xi_1, \xi_2, \xi_3)$  with  $0 \leq \xi_1, \xi_2, \xi_3 \leq 1$ . Further,  $\boldsymbol{\xi}_q$  denotes the Gauss-Legendre quadrature point in the natural coordinate system,  $w_q$  denotes the appropriate quadrature weight and  $\mathbf{J}^{(e)}$  denotes the Jacobian matrix of the mapping of the FE cell from original coordinate system to the natural coordinate system as is usually employed in FE discretization and is assumed to be constant for this discussion. Further,  $F$  in the above is a function of  $\phi_i$  and/or  $\nabla \phi_i$ . The arithmetic complexity and memory footprint associated with the computation in equation (1) can be reduced by exploiting the tensor-structured format of cell-level FE basis functions, which is often the case in FE discretization with the commonly employed hexahedral finite-elements. As an illustration, we consider here the action of FE basis overlap (mass) matrix  $\mathbf{M}$  on the FE discretized vector  $\mathbf{u}$  in 3D i.e.,  $(\mathbf{M}\mathbf{u})_i = \int \sum_j \phi_i(\mathbf{x}) \phi_j(\mathbf{x}) u_j d\mathbf{x}$  where the integral is over the simulation domain which can be recast as  $(\mathbf{M}\mathbf{u})_i = \sum_e (\mathbf{M}\mathbf{u})_i^e = \sum_{q,j} \phi_i(\boldsymbol{\xi}_q) \phi_j(\boldsymbol{\xi}_q) u_j d\mathbf{x}$ . Using the tensor-structured nature of the cell-level FE basis we have  $\phi_i(\boldsymbol{\xi}) = \phi_{i_1}(\xi_1) \phi_{i_2}(\xi_2) \phi_{i_3}(\xi_3)$  and the summation in (1) can be written at the FE cell-level as

$$\begin{aligned} (\mathbf{M}\mathbf{u})_{i_1 i_2 i_3}^{(e)} &= \sum_{q_1 q_2 q_3} \phi_{i_1}(\xi_{q_1}) \phi_{i_2}(\xi_{q_2}) \phi_{i_3}(\xi_{q_3}) w_{q_1} w_{q_2} w_{q_3} \\ &\quad J_{q_1 q_2 q_3} \left[ \sum_{j_1 j_2 j_3} \phi_{j_1}(\xi_{q_1}) \phi_{j_2}(\xi_{q_2}) \phi_{j_3}(\xi_{q_3}) u_{j_1 j_2 j_3} \right] \end{aligned} \quad (2)$$

where the  $i^{\text{th}}$  degree of freedom in 3D is denoted by the multi-index  $i_1 i_2 i_3$  with  $1 \leq i_1, i_2, i_3 \leq p$  where  $p$  denotes the number of FE nodes(grid points) in each direction and we note that for a finite-element interpolating polynomial degree of FEOrder, we have FEOrder =  $p - 1$ . Similarly  $q_1 q_2 q_3$

denotes the multi-index representation of the 3D quadrature point in a given FE cell and further,  $\det(\mathbf{J}^{(e)})$  is denoted by  $J_{q_1 q_2 q_3}$ . Assuming the number of quadrature points also equals  $p$ , the expression in (2) has a computational complexity of  $O(p^4)$  and storage complexity of  $O(p^3)$  as opposed to the cell-level dense matrix-vector approach (see (1)) having a computational complexity and a storage complexity of  $O(p^6)$ .

## III. IMPLEMENTATION METHODOLOGY

We now describe the proposed implementation procedure of accomplishing FE discretized matrix-multivector product using the aforementioned matrix-free approach in the context of the action of FE basis overlap matrix on multivectors. To this end, consider the input node-level multivector  $X$  of size  $N_{vecs} \times N_{dofs}$ , where  $N_{vecs}$  is the number of vectors and  $N_{dofs}$  is the number of degrees of freedom (DoF) corresponding to FE nodes. Note that  $X$  is contiguous in the first index (this convention will be followed throughout the following sections). The proposed implementation comprises of three phases - extraction, cell-level FE-operator action, and assembly. In the extraction step,  $X$  is extracted to form the cell-level multivector  $U$  of size  $N_{vecs} \times p^3 \times N_{cells}$  using a map. Computing the cell-level FE-operator action involves 6 tensor contractions (equations 3 and 5), and an element-wise multiplication with  $J_{q_1 q_2 q_3}$  and  $w_q$  (equation 4). After computing the cell-level FE-operator action, the output  $V$ , the cell-level matrix-multivector product, is assembled back into the output node-level multivector  $Y$  employing the same map used in the extraction phase. Denoting  $P_{jq} = \phi_j(\xi_q)$ , we have the tensor contractions as

$$I_{q_1 q_2 q_3 k} = \sum_{j_1 j_2 j_3} P_{j_1 q_1} P_{j_2 q_2} P_{j_3 q_3} U_{j_1 j_2 j_3 k} \quad (3)$$

$$K_{q_1 q_2 q_3 k} = I_{q_1 q_2 q_3 k} J_{q_1 q_2 q_3} w_{q_1} w_{q_2} w_{q_3} \quad (4)$$

$$V_{i_1 i_2 i_3 k} = \sum_{q_1 q_2 q_3} P_{i_1 q_1} P_{i_2 q_2} P_{i_3 q_3} K_{q_1 q_2 q_3 k} \quad (5)$$

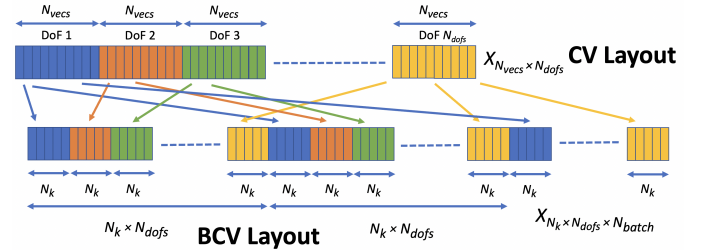


Fig. 1: Depiction of input node-level multivector reshaping to get the Batched Contiguous Vector (BCV) Layout from Contiguous Vector (CV) Layout.

We have explored two layouts for storing the node-level multivector. The first is to store it in the  $N_{vecs} \times N_{dofs}$  layout. This layout will be referred to as the *Contiguous Vector* (CV) layout. The other layout is to reshape the multivector into  $N_k \times N_{dofs} \times N_{batch}$ , as shown in figure 1, where  $N_k$  is chosen according to the FEOrder used and  $N_{batch} = N_{vecs}/N_k$ . This layout will be referred to as the *Batched Contiguous Vector* (BCV) layout.

The BCV layout performs better both on a single CPU core and a single GPU, as evident from sustained performance

shown in figure 2. Under the MPI paradigm, communication is inefficient for the BCV layout because it does not allow communication of all the vectors at a given DoF as a single contiguous data block, unlike the CV layout.

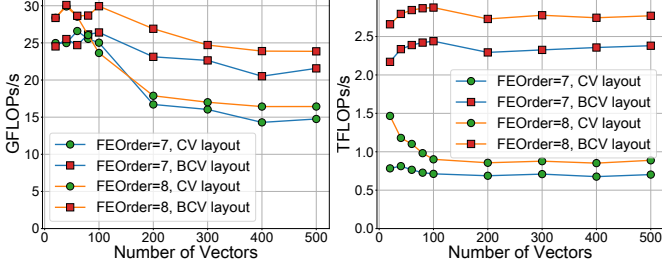


Fig. 2: Sustained Performance of the CV Layout and the BCV Layout on CPUs (left) and GPUs (right). On CPUs, a uniform 3D grid of 27 FE cells was chosen resulting in 10648 DoFs for FEOrder = 7 and 15625 DoFs for FEOrder = 8. On GPUs, a uniform 3D grid of 343 cells was chosen resulting in 125000 DoFs for FEOrder = 7 and 185193 DoFs for FEOrder = 8.

### A. CPU Implementation

We utilize the BCV layout on CPUs as the increased computational efficiency overshadows the communication overhead in this layout. For computing the cell-level FE-operator action, we rewrite each tensor contraction as a matrix-matrix multiplication as described by Deville et al. [18], and use JIT modules from Intel<sup>®</sup> MKL version 2021.2.0 [16] to perform these multiplications. Note that the cell level multivector in the BCV layout is of size  $N_k \times p^3 \times N_{cells} \times N_{batch}$  and the way the matrix multiplications are written allows us to explore various blocking/tiling patterns over both  $N_{batch}$  and  $N_{cells}$  indices. For the problem sizes considered, we found that performing the matrix multiplications in a loop over the  $N_{cells}$  index and the  $N_{batch}$  index without any further tiling shows the best performance. We also note that extraction and assembly for the cell level vector for each batch allow us to maintain cache locality.

### B. GPU Implementation

We utilize the CV layout on GPUs as the increased communication overhead in the BCV layout overshadows its computational gains. For the matrix-matrix multiplication (similar to CPUs) involved in computing the cell-level FE-operator action, we find that a naive shared memory implementation performs better than cuBLAS dgemm modules, as it avoids multiple reads from and writes to the global memory.

The three steps in matrix-free multiplication are performed in a single kernel launch to reduce data movement and device memory accesses. This kernel does not explicitly construct the cell level multivectors  $U$  and  $V$  in the device memory, further reducing memory footprint. We find that tiling over the number of vectors with tile length  $N_s$  allows us to fill the static shared memory to the default limit. The kernel is launched with a 2-D grid of  $N_{cells} \times N_{tiles}$  threadblocks where  $N_{tiles} = N_{vecs}/N_s$ . The threadblocks are launched with  $N_s$  threads in the x-direction. In the y-direction, the threads handle the rows of the second matrix involved in the multiplication.

The choice of  $N_s$  and the number of threads launched in the y-direction, both depend on the FEOrder of the problem.

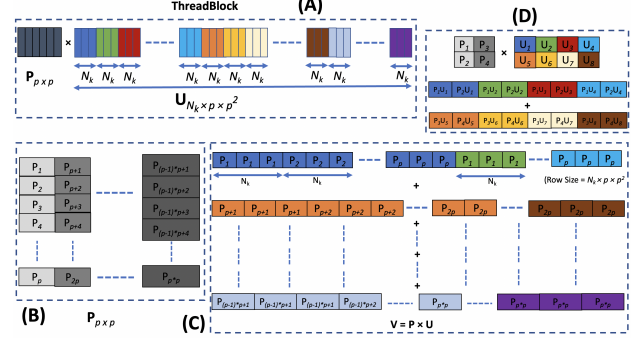


Fig. 3: Depiction of the compute step per thread block. (A): Tensor contraction in a threadblock. (B): Layout used for the matrix  $P$ . (C): Tensor contraction as linear combination of columns of  $P$ . (D): Cell-level FE-Operator Action with  $p = 2$  as an example.

In the cell-level FE-operator action step, the matrix multiplications are executed as linear combinations of columns of the shape function  $P$  matrix as described in figure 3.  $N_s$  is chosen such that  $P_{p \times p}$  and  $U_{p \times p^2 \times N_s}$  can fit in the shared memory allowing  $P$  to be reused for the subsequent tensor contractions. The matrix  $P$  is read into the shared memory and then the first tensor contraction is started as soon as first element of matrix  $U$  is read from the device memory. This allows us to utilize each data access to its full compute potential and avoid rereading the same data. Furthermore, as each thread accesses the same values from the  $P$  matrix, the accesses get broadcasted, which helps reduce bank conflicts in shared memory. To further improve performance, registers are utilized to keep the data local to each thread as much as possible. This reduces data movement even from shared memory and better utilizes the hardware. Finally, in the assembly step `atomicAdd` is used to avoid race conditions and safely assemble the output node-level multivector  $Y$ .

## IV. RESULTS

The CPU performance and timings were collected on Intel<sup>®</sup> Xeon Gold 6248R CPUs, and the GPU performance analysis was done on Tesla V100-SXM2-32 GB. Each measurement was repeated 100 times and averaged. In this section, FEOrder = 7 and 8 were chosen for assessing the performance of the proposed implementation procedure on CPUs and GPUs.

The proposed matrix-free implementation is benchmarked against the cell-matrix method which is implemented by utilizing the `dgemm_batch_strided` from Intel<sup>®</sup> MKL version 2021.2.0 on CPUs and `cublasDgemmStridedBatched` CUDA 11.0 on GPUs for computing the  $H_{p^3 \times p^3} \times U_{p^3 \times N_{vecs}}$  dense matrix-matrix product for every cell. Note that  $H$  in this study represents the cell-level FE basis overlap matrix. Further, our matrix-free implementation is compared with the existing matrix-free implementation in `deal.II` library [7]. We extend the `deal.II` library to work with multivectors using a naive `for` loop over  $N_{vecs}$  since `deal.II` does not provide data structures to handle multivectors directly.

## A. CPU

We studied the performance for the BCV layout by varying the batch size  $N_k$ , and it was observed that best performance is achieved for a batch size of around  $N_k = 20$  for all the FEOrders and problem sizes considered.

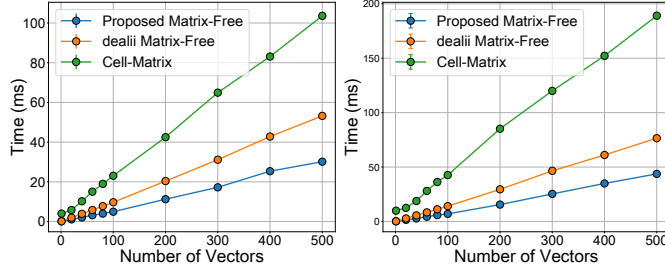


Fig. 4: Timings for FEOrder=7 (left) and FEOrder=8 (right) on a single CPU core (1 MPI task). A uniform 3D grid of 27 cells was chosen, resulting in 10648 DoFs for FEOrder=7 and 15625 DoFs for FEOrder=8

Figure 4 demonstrates that on a single CPU core, our CPU matrix-free implementation for the mass matrix performs better than the cell-matrix method and the `dealii` matrix-free implementation. In the 100 vector case, we achieved 4.7x and 6.1x speedups over the cell-matrix route for FEOrders 7 and 8, respectively. For the same case, 2.0x speedup over the `dealii` implementation was achieved for both FEOrders 7 and 8.

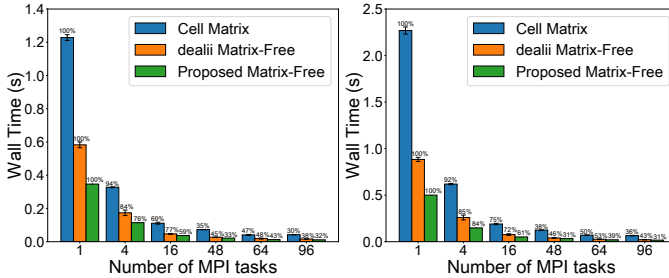


Fig. 5: Strong scaling study for the 3 implementations for FEOrder=7 (left) and FEOrder=8 (right). A uniform 3D grid of 512 cells was chosen resulting in 185193 DoFs for FEOrder=7 and 274625 DoFs for FEOrder=8. The number of vectors was chosen to be 300.

The strong scaling studies in figure 5 demonstrate the scalability of our implementation.

## B. GPU

To optimize the shared memory implementation, tiling over  $N_{vecs}$  is explored and  $N_s$  (`blockDim.x`) is determined for best performance. We also vary `blockDim.y` in multiples of 32 (as warp size is 32) to test for best performance.

The final analysis was done using the best implementation for each FEOrder:  $N_s = 5$  for FEOrder = 7 and  $N_s = 4$  for FEOrder = 8. The map is accessed from the device memory for both FEOrders to save space in shared memory. Static shared memory implementation was used for both FEOrders to work in the default shared memory limit of 48 kB (for the V100 GPU) as it was faster than increasing the shared memory through dynamic shared memory method.

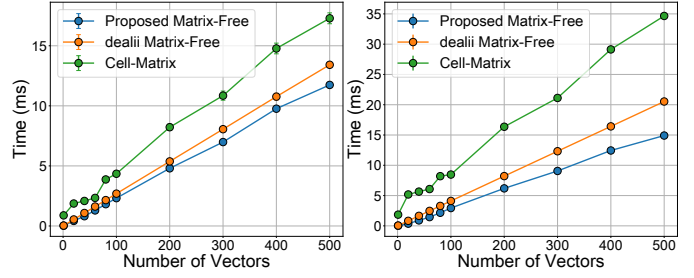


Fig. 6: Timings for FEOrder=7 (left) and FEOrder=8 (right) on a single GPU using a single MPI task. A uniform 3D grid of 343 cells was chosen resulting in 125000 DoFs for FEOrder=7 and 185193 DoFs for FEOrder=8.

Figure 6 demonstrates that on a single GPU, our GPU matrix-free implementation for the mass matrix is faster than the cell-matrix method and the `dealii` matrix-free implementation. In the 100 vector case, we achieved 1.9x and 2.9x speedups over the cell-matrix route for FEOrders 7 and 8, respectively. For the same case, we achieved 1.2x and 1.4x speedups over the `dealii` implementation for FEOrders 7 and 8, respectively.

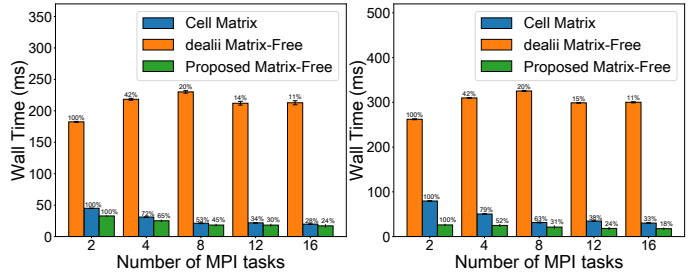


Fig. 7: Strong scaling study for the 3 implementations for FEOrder=7 (left) and FEOrder=8 (right). A uniform 3D grid of 1728 cells was chosen resulting in 614125 DoFs for FEOrder=7 and 912673 DoFs for FEOrder=8. The number of vectors was chosen to be 300.

Figure 7 demonstrates the scalability of our implementation on GPUs. The large wall times of the `dealii` implementation are because of discontinuous MPI communications resulting from having to call the `dealii` single vector routine in a `for` loop.

## V. CONCLUSIONS

In conclusion, we have illustrated and implemented an efficient matrix-free algorithm for mass matrix multivector multiplication. We have also shown significant speedups our implementation provides compared to the traditional cell-matrix method. We also note that our matrix multivector multiplication implementation is significantly more efficient than the `dealii` matrix-free implementation and the cell-matrix method.

The future work involves comparing our implementation to the matrix-free implementation in MFEM [8]. We also intend to extend the implementation to work with the Laplacian, Helmholtz, and quantum-mechanical Hamiltonian operators arising in Kohn-Sham density functional theory (DFT) calculations in DFT-FE [3].

## REFERENCES

- [1] G. F. Carey, E. Barragy, R. McLay, and M. Sharma, "Element-by-element vector and parallel computations," *Communications in Applied Numerical Methods*, vol. 4, no. 3, pp. 299–307, 5 1988. [Online]. Available: <https://onlinelibrary.wiley.com/doi/10.1002/cnm.1630040303>
- [2] P. Motamarri, S. Das, S. Rudraraju, K. Ghosh, D. Davydov, and V. Gavini, "DFT-FE – A massively parallel adaptive finite-element code for large-scale density functional theory calculations," *Computer Physics Communications*, vol. 246, p. 106853, 1 2020. [Online]. Available: <https://linkinghub.elsevier.com/retrieve/pii/S0010465519302309>
- [3] S. Das, P. Motamarri, V. Subramanian, D. M. Rogers, and V. Gavini, "DFT-FE 1.0: A massively parallel hybrid CPU-GPU density functional theory code using finite-element discretization," *Computer Physics Communications*, vol. 280, p. 108473, 11 2022. [Online]. Available: <https://linkinghub.elsevier.com/retrieve/pii/S0010465522001928>
- [4] K. Ljungkvist, "Matrix-Free Finite-Element Computations On Graphics Processors with Adaptively Refined Unstructured Meshes," in *25th High Performance Computing Symposium (HPC 2017)*, vol. 49, no. 3. Society for Modeling and Simulation International (SCS), 2017, pp. 1–12. [Online]. Available: <http://dl.acm.org/citation.cfm?id=3108097>
- [5] M. Kronbichler and K. Kormann, "A generic interface for parallel cell-based finite element operator application," *Computers & Fluids*, vol. 63, pp. 135–147, 6 2012. [Online]. Available: <https://linkinghub.elsevier.com/retrieve/pii/S0045793012001429>
- [6] D. Davydov, J. Pelteret, D. Arndt, M. Kronbichler, and P. Steinmann, "A matrix-free approach for finite-strain hyperelastic problems using geometric multigrid," *International Journal for Numerical Methods in Engineering*, vol. 121, no. 13, pp. 2874–2895, 7 2020. [Online]. Available: <https://onlinelibrary.wiley.com/doi/10.1002/nme.6336>
- [7] D. Arndt, W. Bangerth, D. Davydov, T. Heister, L. Heltai, M. Kronbichler, M. Maier, J.-P. Pelteret, B. Turcksin, and D. Wells, "The deal.II finite element library," 2019. [Online]. Available: <https://www.dealii.org/>
- [8] R. Anderson, J. Andrej, A. Barker, J. Bramwell, J. S. Camier, J. Cerveny, V. Dobrev, Y. Dudouit, A. Fisher, T. Kolev, W. Pazner, M. Stowell, V. Tomov, I. Akkerman, J. Dahm, D. Medina, and S. Zampini, "MFEM: A modular finite element methods library," *Computers & Mathematics with Applications*, vol. 81, pp. 42–74, 1 2021.
- [9] J. Brown, A. Abdelfattah, V. Barra, N. Beams, J.-S. Camier, V. Dobrev, Y. Dudouit, L. Ghaffari, T. Kolev, D. Medina, W. Pazner, T. Ratnayaka, J. Thompson, and S. Tomov, "libCEED: Fast algebra for high-order element-based discretizations," *Journal of Open Source Software*, vol. 6, no. 63, p. 2945, 7 2021.
- [10] T. J. R. Hughes, *The Finite Element Method: Linear Static and Dynamic Finite Element Analysis*, ser. Dover Civil and Mechanical Engineering. Dover Publications, 2012. [Online]. Available: [https://books.google.co.in/books?id=cHH2n\\_qBK0IC](https://books.google.co.in/books?id=cHH2n_qBK0IC)
- [11] E. Tsuchida and M. Tsukada, "Adaptive finite-element method for electronic-structure calculations," *Physical Review B - Condensed Matter and Materials Physics*, vol. 54, no. 11, pp. 7602–7605, 1996.
- [12] K. Ghosh, H. Ma, V. Gavini, and G. Galli, "All-electron density functional calculations for electron and nuclear spin interactions in molecules and solids," *Physical Review Materials*, vol. 3, no. 4, p. 043801, 4 2019. [Online]. Available: <https://link.aps.org/doi/10.1103/PhysRevMaterials.3.043801>
- [13] S. Markidis, "The Old and the New: Can Physics-Informed Deep-Learning Replace Traditional Linear Solvers?" *Frontiers in Big Data*, vol. 4, 11 2021.
- [14] D. Davydov and M. Kronbichler, "Algorithms and Data Structures for Matrix-Free Finite Element Operators with MPI-Parallel Sparse Multi-Vectors," *ACM Transactions on Parallel Computing*, vol. 7, no. 3, 7 2020. [Online]. Available: <http://arxiv.org/abs/1907.01005>
- [15] N. Beams, A. Abdelfattah, S. Tomov, J. Dongarra, T. Kolev, and Y. Dudouit, "High-Order Finite Element Method using Standard and Device-Level Batch GEMM on GPUs," in *Proceedings of Scala 2020: 11th Workshop on Latest Advances in Scalable Algorithms for Large-Scale Systems, Held in conjunction with SC 2020: The International Conference for High Performance Computing, Networking, Storage and Analysis*, 2020, pp. 53–60.
- [16] G. Fedorov and L. Huot, "Intel® Math Kernel Library Improved Small Matrix Performance Using Just-in-Time (JIT) Code Generation for Matrix Multiplication (GEMM)." [Online]. Available: <https://www.intel.com/content/www/us/en/developer/articles/technical/onekl-improved-small-matrix-performance-using-just-in-time-jit-code.html>
- [17] A. Heinecke, G. Henry, M. Hutchinson, and H. Pabst, "LIBXSMM: Accelerating Small Matrix Multiplications by Runtime Code Generation," in *SC16: International Conference for High Performance Computing, Networking, Storage and Analysis*, vol. 0. IEEE, 11 2016, pp. 981–991. [Online]. Available: <https://ieeexplore.ieee.org/document/7877162/>
- [18] M. O. Deville, P. F. Fischer, and E. H. Mund, *High-Order Methods for Incompressible Fluid Flow*. Cambridge University Press, 8 2002. [Online]. Available: <https://www.cambridge.org/core/product/identifier/9780511546792/type/book>